

Article

# Backhaul-Aware Resource Allocation and Optimum Placement for UAV-Assisted Wireless Communication Network

Yishi Xue <sup>1,2</sup>, Bo Xu <sup>1,2</sup>, Wenchao Xia <sup>1,2</sup>, Jun Zhang <sup>1,2</sup> and Hongbo Zhu <sup>1,2,\*</sup>

<sup>1</sup> Jiangsu Key Laboratory of Wireless Communications, Nanjing University of Posts and Telecommunications, Nanjing 210003, China; 2015010204@njupt.edu.cn (Y.X.); 1018010321@njupt.edu.cn (B.X.); 2015010203@njupt.edu.cn (W.X.); zhangjun@njupt.edu.cn (J.Z.)

<sup>2</sup> Engineering Research Center of Health Service System Based on Ubiquitous Wireless Networks, Ministry of Education, Nanjing University of Posts and Telecommunications, Nanjing 210003, China

\* Correspondence: hbz@njupt.edu.cn

Received: 19 July 2020; Accepted: 25 August 2020; Published: 28 August 2020



**Abstract:** Driven by its agile maneuverability and deployment, the unmanned aerial vehicle (UAV) becomes a potential enabler of the terrestrial networks. In this paper, we consider downlink communications in a UAV-assisted wireless communication network, where a multi-antenna UAV assists the ground base station (GBS) to forward signals to multiple user equipments (UEs). The UAV is associated with the GBS through in-band wireless backhaul, which shares the spectrum resource with the access links between UEs and the UAV. The optimization problem is formulated to maximize the downlink ergodic sum-rate by jointly optimizing UAV placement, spectrum resource allocation and transmit power matrix of the UAV. The deterministic equivalents of UE's achievable rate and backhaul capacity are first derived by utilizing large-dimensional random matrix theory, in which, only the slowly varying large-scale channel state information is required. An approximation problem of the joint optimization problem is then introduced based on the deterministic equivalents. Finally, an algorithm is proposed to obtain the optimal solution of the approximate problem. Simulation results are provided to validate the accuracy of the deterministic equivalents, and the effectiveness of the proposed method.

**Keywords:** UAV placement; resource allocation; in-band wireless backhaul; large random matrix theory; regularized zero-forcing precoding

## 1. Introduction

Recently, unmanned aerial vehicles (UAVs) has been widely investigated and applied to provide seamless coverage and capacity enhancement in wireless communication systems [1–3]. Deployed as aerial base stations or mounted with access points, UAVs can provide flexible and on-demand services to ground users dynamically by leveraging its agile mobility and maneuverability. As typical applications, UAVs can be exploited to load traffic in temporary or unexpected circumstances when the ground base stations (GBSs) are congested or broken. UAVs can also assist the GBSs to relay signals to remote users who are out of the coverage provided by terrestrial infrastructure [4].

In the UAV-assisted networks, wireless backhaul and cellular-connected UAVs have been proposed as potential solutions to connect UAV networks with terrestrial networks [5]. However, differing from the GBSs, the lack of fixed backhaul link for UAVs has emerged as a challenge in UAV-assisted wireless communication network, which needs to be further investigated [6]. In addition, an efficient resource allocation strategy is essential to improve the resource utilization and

to enhance the system capacity among UEs' access links and UAV's backhaul links in the UAV-assisted networks [7].

The main characteristic of the UAV applications in wireless communication system is agile deployment. Therefore, the placement and trajectory optimization of the UAVs have been researched in consideration of the quality of access links of user equipments (UEs). In Reference [8], the minimum throughput of all UEs was maximized by jointly optimizing UEs' scheduling and association along with UAVs' power control and trajectory. In Reference [9], the authors minimized the total UAV energy consumption with both propulsion and communication related energy by jointly optimizing the UAV's trajectory, communication time allocation, and the total mission completion time. The optimum placement of a relaying UAV was studied in Reference [10] to maximum reliability for both static and mobile UAVs. In Reference [11], the optimum placement was considered to minimize the number of UAVs and the system cost while guaranteeing the wireless coverage performance.

However, in the UAV-assisted wireless communication network, the signals of UEs are forwarded through the wireless backhaul links between the UAV and the GBS, thus, the limited backhaul capacity would degrade the overall system performance [7]. Meanwhile, the spectrum efficiency of UEs' access links and UAV's backhaul links can be both affected by the placement of the UAVs. To this end, the optimal placement of UAV in the UAV-assisted network requires to consider both access and backhaul links. In some existing works, the out-band wireless backhaul is considered. In Reference [12], the millimeter wave frequency band is adopted for UAVs, and the microwave frequency band is adopted for GBSs. However, the dedicated spectrum band for backhaul link may be unavailable when the spectrum resources are limited. Therefore, the in-band backhaul link can be adopted where the spectrum resources are shared among UEs' access links and UAV's backhaul links. However, sharing of spectrum resources among access and backhaul links may induce additional interference. The orthogonal time-frequency resource allocation and user scheduling are effective methods to mitigate the interference [8,13,14]. Different from a number of previous studies where the UAV was equipped with single antenna, the multi-antenna UAV was considered in References [15–17] to form an MIMO communication link.

The multi-antenna UAV has rarely been analyzed in the UAV-assisted wireless communication network with the consideration of the in-band backhaul link. With the precoding method performed, the UAV can serve multiple UEs simultaneously, meanwhile, the inter-user interference can be well mitigated. Benefiting from the large-dimensional random matrix theory, the deterministic equivalents can be obtained without requiring the instantaneous channel state information. Therefore, the system performance in regard to different variables will be numerically analyzed avoiding Monte Carlo averaging which leads to high computational complexity. In addition, once the locations of UEs are determined, the optimal UAV placement as well as the spectrum resource allocation between the backhaul and access links can be pre-designated which can maximize the network throughput.

In this paper, we aim to maximize the downlink ergodic sum-rate by jointly optimizing UAV placement, spectrum resource allocation and transmit power matrix of the UAV. The composite channel model proposed in Reference [15] is adopted which considers both large-scale and small-scale fading. The Rayleigh small-scale fading is taken into account in accord with low-altitude UAV scenario [18]. Note that computing the ergodic sum-rate relies on the instantaneous channel state information, which may lead to prohibitively computational complexity. Motivated by this challenge, the large-dimensional random matrix theory [19–21] is utilized to derive the deterministic equivalents of UE's achievable rate and UAV's backhaul capacity, which relies on only statistical channel information. In this paper, we adopt regularized zero-forcing (RZF) precoding to mitigate inter-user interference [22]. The main contributions of this paper are summarized as follows.

- First, we consider the downlink transmission in a UAV-assisted wireless communication network. Differing from previous works, a multi-antenna UAV is considered to assist a multi-antenna GBS to forward signals for remote UEs which are out of the coverage provided from the GBS. The UAV

is connected to the GBS through in-band wireless backhaul link, which shares the spectrum resource with the access links of UEs as the spectrum resource is limited.

- Next, we consider a composite channel model in which both large-scale and small-scale channel fading are considered. The RZF precoding is performed across the transmitted signals at the UAV to mitigate inter-user interference. In addition, to mitigate the computational complexity, we introduce the large-dimensional random matrix theory and derive the deterministic equivalents of UE's achievable rate and UAV's backhaul capacity which depends on only slowly-varying statistical channel information. The accuracy of the deterministic equivalents is verified.
- Last, we formulate an optimization problem to maximize the downlink network sum-rate of UEs by jointly optimizing UAV placement, spectrum resource allocation and the transmit power matrix of the UAV. Based on the deterministic equivalents, an approximation problem of the joint optimization problem is proposed, from which the optimal solution of the approximation problem can be obtained. The effectiveness of the proposed method is also validated by simulations.

The remainder of this paper is organized as follows. In Section 2, the system model is described and the optimization problem is formulated. In Section 3, the deterministic equivalents of the ergodic rates is derived. In Section 4, we propose the algorithms to solve the approximate problem based on the deterministic results. In Section 5, simulation results for the proposed methods are provided, and the conclusion is drawn in Section 6.

Notation: In this paper, vectors, and matrices are denoted by lower-case, and upper-case bold-face letters, respectively. The  $N \times N$  identity matrix is denoted by  $\mathbf{I}_N$ . The superscripts  $(\cdot)^H$ ,  $(\cdot)^T$ , and  $(\cdot)^*$  represent the conjugate-transpose, transpose, and conjugate operations, respectively.  $\mathbb{E}\{\cdot\}$  is used to denote expectation with respect to all random variables within the brackets. The matrix principal square root, inverse, trace, and determinant are represented by  $(\cdot)^{\frac{1}{2}}$ ,  $(\cdot)^{-1}$ ,  $\text{tr}(\cdot)$ , and  $\det(\cdot)$ , respectively.

## 2. System Model and Problem Formulation

As shown in Figure 1, a downlink UAV-assisted wireless communication network is considered, consisting of an  $N$ -antenna GBS and a rotary-wing UAV equipped with  $M$  antennas. The UAV is connected to the GBS through in-band wireless backhaul link. The UAV acting as a remote relay, assists the GBS to forward signals for  $K$  UEs in remote areas outside the coverage of the GBS. The UEs have a single antenna each and they simultaneously receive messages from the UAV.

We assume the messages sent to the UEs cannot be transmitted by the GBS directly due to blockage and far distance. The messages for UEs are received by the UAV first and then relayed to UEs. We consider the wireless backhaul link between the UAV and the GBS is in-band along with the UEs' access links. In the frequency domain, the dynamic allocation of bandwidth resource for wireless backhaul and user communication is adopted. We assume that the total available bandwidth for the whole network is  $F$  Hz, from which is divided into two orthogonal parts  $F_1 = \eta F$  and  $F_2 = F - F_1$ , where  $\eta \in [0, 1]$  is a scale factor. The former is designated to the UAV to serve the UEs and the latter is designed to the backhaul link.

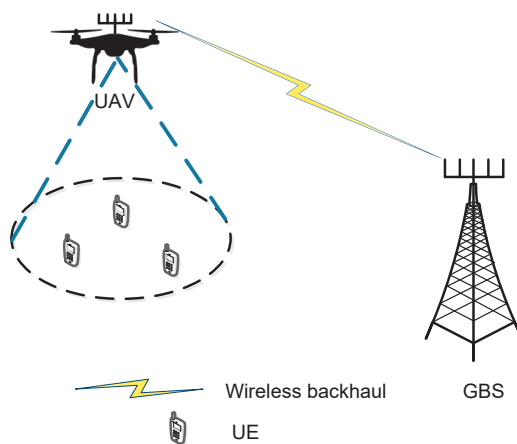


Figure 1. System architecture of a UAV-assisted wireless communication network.

2.1. Transmission Model under Polar Coordinate

According to a three-dimensional Cartesian coordinate system, we consider the GBS is located at the origin  $(0,0,0)$ . The UAV flies at a fixed altitude of  $l$  m. The distance between the projection of the UAV on the ground and the GBS is denoted as  $r$ . The UAV flies to a dispatched position and then hovers to transmit data for a group of  $K$  UEs. The polar coordinate of UE  $k$  with respect to the origin is denoted as  $(z_k, \theta_k, 0)$ , thus, the corresponding cartesian coordinate is  $(z_k \cos \theta_k, z_k \sin \theta_k, 0)$ . The azimuth angle of the UAV’s projection with respect to the horizontal axis is set as [15]

$$\phi = \frac{1}{K} \sum_{k=1}^K \theta_k. \tag{1}$$

Thus, the cartesian coordinate of the position at which the UAV hovers is expressed as  $(r \cos \phi, r \sin \phi, l)$ . As the downlink transmission from the UAV to the served UEs is considered, the distance between the UAV and UE  $k$  is denoted as

$$d_k = \sqrt{r^2 + z_k^2 + l^2 - 2rz_k \cos(\phi - \theta_k)}. \tag{2}$$

Considering low-altitude UAV scenario [18], the UAV-ground channels contain some multi-path components due to reflection and scattering. We take into account both the large-scale and the small-scale channel fading. The channel between the UAV and UE  $k$  is defined as  $\mathbf{h}_k = \sqrt{\beta d_k^{-\alpha}} \tilde{\mathbf{h}}_k$ , where  $\beta$  denotes the channel power gain at the reference distance  $1m$ ,  $\alpha$  denotes the path loss exponent between the UAV and UE  $k$ , and  $\tilde{\mathbf{h}}_k \in \mathbb{C}^M$  accounts for the small-scale fading which has independent and identically distributed (i.i.d.) zero-mean entries of unit variance.

We assume the channel state information is available in the considered system. The received signal  $y_k$  of UE  $k$  from the UAV is given by

$$y_k = \mathbf{h}_k^H \mathbf{w}_k s_k + \sum_{j=1, j \neq k}^K \mathbf{h}_k^H \mathbf{w}_j s_j + n_k, \tag{3}$$

where  $\mathbf{w}_k \in \mathbb{C}^M$  is the precoding matrix for UE  $k$ ,  $s_k \sim \mathcal{CN}(0, 1)$  denotes the transmitted symbols for UE  $k$ , and  $n_k \sim \mathcal{CN}(0, \sigma^2)$  is the additive white Gaussian noise (AWGN) at the receiver. We define  $\mathbf{W} = [\mathbf{w}_1, \mathbf{w}_2, \dots, \mathbf{w}_K] \in \mathbb{C}^{M \times K}$  as the precoding matrix for all UEs, and  $\mathbf{H} = [\mathbf{h}_1, \mathbf{h}_2, \dots, \mathbf{h}_K] \in \mathbb{C}^{M \times K}$  as the channel matrix which collects the channels between all the UEs and the UAV.  $\mathbf{H}$  is modeled as

$$\mathbf{H} = \tilde{\mathbf{H}} \sqrt{\mathbf{D}}, \tag{4}$$

where  $\tilde{\mathbf{H}} = [\tilde{\mathbf{h}}_1, \tilde{\mathbf{h}}_2, \dots, \tilde{\mathbf{h}}_K] \in \mathbb{C}^{M \times K}$  accounts for small-scale fading, and  $\mathbf{D}$  is a  $K \times K$  diagonal matrix whose diagonal elements  $\beta d_k^{-\alpha}$ 's denote large-scale channel fading. Here, the RZF precoder is considered [22], and given by

$$\mathbf{W} = \zeta(\mathbf{H}\mathbf{H}^H + \omega\mathbf{I}_M)^{-1}\mathbf{H}\sqrt{\mathbf{P}^{(U)}} = \hat{\mathbf{W}}\sqrt{\mathbf{P}^{(U)}}, \tag{5}$$

where  $\mathbf{P}^{(U)} \in \mathbb{R}^{K \times K}$  is a diagonal matrix of transmit power at the UAV whose  $k$ -th element is  $p_k^{(U)}$ ,  $\omega$  is the regularization scalar, and  $\zeta$  is a normalization scalar satisfying

$$\zeta^2 = \frac{1}{\text{tr} \left[ (\mathbf{H}\mathbf{H}^H + \omega\mathbf{I}_M)^{-1} \mathbf{H}\mathbf{H}^H (\mathbf{H}\mathbf{H}^H + \omega\mathbf{I}_M)^{-1} \right]}. \tag{6}$$

The normalized ergodic sum-rate of UEs is given as

$$\begin{aligned} R_{\text{sum}} &= \eta R_{0,\text{sum}} \\ &= \eta \sum_{k=1}^K \mathbb{E}_{\mathbf{H}} [\log_2 (1 + \gamma_k)], \end{aligned} \tag{7}$$

where  $\gamma_k$  is the received signal to interference plus noise ratio (SINR) of UE  $k$ , which is expressed as

$$\gamma_k = \frac{p_k^{(U)} |\mathbf{h}_k^H \hat{\mathbf{w}}_k|^2}{\sum_{j=1, j \neq k}^K p_j^{(U)} |\mathbf{h}_k^H \hat{\mathbf{w}}_j|^2 + \sigma^2}. \tag{8}$$

The location of the GBS is considered at the origin of the coordinate system, thus, the distance between the UAV and the GBS is denoted as  $d_u = \sqrt{r^2 + l^2}$ . The UAV receives the UEs' messages from the GBS through wireless backhaul link. The large-scale and the small-scale channel fading elements between the GBS and the UAV are both considered. We denote the channel from the GBS to the UAV through wireless backhaul link as  $\mathbf{G} \in \mathbb{C}^{M \times N}$ , which is given by

$$\mathbf{G} = \sqrt{\beta d_u^{-\alpha}} \tilde{\mathbf{G}}, \tag{9}$$

where  $\tilde{\mathbf{G}} \in \mathbb{C}^{M \times N}$  accounts for the small-scale fading channel in which the elements are i.i.d. complex random variables with zero mean and unit variance, and  $\alpha$  denotes the path loss exponent from the GBS to the UAV. The received signal  $\mathbf{y}_u \in \mathbb{C}^M$  at the UAV from the GBS through wireless backhaul link can be expressed as

$$\mathbf{y}_u = \mathbf{G} \sqrt{\mathbf{P}^{(B)}} \mathbf{s}_u + \mathbf{n}_u, \tag{10}$$

where  $\mathbf{s}_u \in \mathbb{C}^N \sim \mathcal{CN}(0, \mathbf{I}_N)$  is the signal vector transmitted from the GBS, the diagonal matrix  $\mathbf{P}^{(B)}$  denotes the transmit power allocation at the GBS, and  $\mathbf{n}_u \sim \mathcal{CN}(0, \sigma^2 \mathbf{I}_M)$  is the independent AWGN. The normalized ergodic capacity rate of the backhaul link from the GBS to the UAV can be expressed as  $R_{\text{bh}}$

$$\begin{aligned} R_{\text{bh}} &= (1 - \eta) R_{0,\text{bh}} \\ &= (1 - \eta) \mathbb{E}_{\mathbf{G}} \left( \log_2 \left| \frac{1}{\sigma^2} \mathbf{G} \mathbf{P}^{(B)} \mathbf{G}^H + \mathbf{I}_M \right| \right). \end{aligned} \tag{11}$$

### 2.2. Problem Formulation

In the considered UAV-assisted network, by jointly designing the spectrum resource allocation factor  $\eta$ , the UAV projection distance  $r$ , and the transmit power matrix at the UAV  $\mathbf{P}^{(U)}$ , the achievable ergodic sum-rate maximization problem can be formulated as

$$\max_{\eta, r, \mathbf{P}^{(U)}} R_{\text{sum}} \tag{12a}$$

$$\text{s.t. } \eta R_{0,\text{sum}} \leq (1 - \eta) R_{0,\text{bh}}, \tag{12b}$$

$$0 \leq \eta \leq 1, \tag{12c}$$

$$r \geq 0, \tag{12d}$$

$$\text{tr}(\mathbf{P}^{(U)}) \leq P_{\text{max}}^{(U)}, \tag{12e}$$

where the constraint (12b) indicates the sum-rate of UEs is restricted by the wireless backhaul capacity since the signals transmitted to all UEs are first received by the UAV through wireless backhaul. The constraint (12e) describes the transmit power constraint for the UAV. Noting that the optimization problem is based on the ergodic sum-rate, Monte Carlo averaging over channels is time-consuming and compute-complicated. Moreover, the small-scale channel fading is difficult to acquire during the UAV's flight. Therefore, the deterministic equivalents of the ergodic sum-rate and wireless backhaul capacity in the large-system regime are introduced, and the optimization problem can be solved based on the approximations in the following sections.

### 3. Deterministic Equivalent

In this section, we derive the deterministic equivalents of  $R_{\text{sum}}$  and  $R_{\text{bh}}$  in the large-system regime where  $N$ ,  $M$ , and  $K$  are assumed to approach infinity with the ratio  $M/N$  and  $K/M$  fixed.

#### 3.1. Deterministic Equivalent of $R_{\text{sum}}$

The following lemma is provided to give the deterministic equivalent  $\bar{\gamma}_k$  of the SINR  $\gamma_k$  by mean of large dimensional random matrix theory tools.

**Lemma 1.** We assume that  $\frac{1}{M} \mathbf{H} \mathbf{H}^H$  has uniformly bounded spectral norm with respect to  $M$ . Therefore, we have  $\gamma_k - \bar{\gamma}_k \rightarrow 0$  almost surely as  $M \rightarrow \infty$ , where

$$\bar{\gamma}_k = \frac{p_k^{(U)} e_k^2}{\bar{\chi}_k + \sigma^2 \bar{\delta} (1 + e_k)^2}, \tag{13}$$

with

$$\bar{\chi}_k = \frac{\beta}{d_k^\alpha M} \sum_{j=1, j \neq k}^K p_j^{(U)} \frac{e'_j}{(1 + e_j)^2}, \tag{14}$$

$$\bar{\delta} = \frac{1}{M} \sum_{k=1}^K \frac{e'_k}{(1 + e_k)^2}. \tag{15}$$

$e_k$  forms the unique solution of the following equations

$$e_k = \frac{\beta}{d_k^\alpha M} \text{tr}(\mathbf{\Psi}), \tag{16a}$$

$$\mathbf{\Psi} = \left( \frac{1}{M} \sum_{k=1}^K \frac{\beta}{d_k^\alpha (1 + e_k)} \mathbf{I}_M + \omega \mathbf{I}_M \right)^{-1}. \tag{16b}$$

Define  $\mathbf{e}' = [e'_1, \dots, e'_k]^T$  where the term  $e'_k$  is the derivative of  $e_k$ ,  $\mathbf{J}$ , and  $\mathbf{v}$  as

$$[\mathbf{J}]_{k,j} = \frac{\beta^2}{M^2 d_k^\alpha d_j^\alpha (1 + e_j)^2} \text{tr}(\mathbf{\Psi}^2), \tag{17}$$

$$\mathbf{v} = \left[ \frac{\beta}{d_1^\alpha M} \text{tr}(\mathbf{\Psi}^2), \dots, \frac{\beta}{d_k^\alpha M} \text{tr}(\mathbf{\Psi}^2) \right]^T. \tag{18}$$

Therefore,  $\mathbf{e}'$  is given explicitly as

$$\mathbf{e}' = (\mathbf{I}_K - \mathbf{J})^{-1} \mathbf{v}. \tag{19}$$

**Proof.** Refer to Appendix A.  $\square$

Utilizing the continuous mapping theorem and the deterministic equivalent of  $\gamma_k$ , we obtain  $\log_2(1 + \gamma_k) - \log_2(1 + \tilde{\gamma}_k) \rightarrow 0$  as  $M \rightarrow \infty$ . Therefore, the deterministic equivalent of the normalized ergodic sum-rate  $R_{\text{sum}}$  is given by  $\bar{R}_{\text{sum}} = \eta \bar{R}_{0,\text{sum}}$  with  $\bar{R}_{0,\text{sum}} = \sum_{k=1}^K \log_2(1 + \tilde{\gamma}_k)$ .

### 3.2. Deterministic Equivalent of $R_{\text{bh}}$

According to Reference [23], the following lemma is provided to give the deterministic equivalent of the normalized backhaul ergodic rate  $R_{\text{bh}}$ .

**Lemma 2.** Consider that the elements of  $\mathbf{G}$  are i.i.d. complex Gaussian variables with independent real and imaginary parts. For brevity, the transmit power budget at the GBS is assumed to be  $p_b$ . Therefore, we have  $R_{\text{bh}} - \bar{R}_{\text{bh}} \rightarrow 0$  almost surely as  $M \rightarrow \infty$ .  $\bar{R}_{\text{bh}} = (1 - \eta) \bar{R}_{0,\text{bh}}$ , and

$$\bar{R}_{0,\text{bh}} = \frac{1}{\log 2} (\Delta - \log |\sigma^2 \mathbf{I}_M|), \tag{20}$$

where

$$\Delta = \log |\mathbf{Y}| + N \left( \frac{1}{1 + \varphi} - \log \frac{1}{1 + \varphi} - 1 \right), \tag{21}$$

with

$$\varphi = \frac{p_b \beta}{d_u^\alpha} \text{tr}(\mathbf{Y}^{-1}), \tag{22a}$$

$$\mathbf{Y} = \left( \frac{N p_b \beta}{d_u^\alpha (1 + \varphi)} + \sigma^2 \right) \mathbf{I}_M. \tag{22b}$$

**Proof.** Refer to Appendix B.  $\square$

The deterministic equivalents  $\bar{R}_{\text{sum}}$  and  $\bar{R}_{\text{bh}}$  are determined by statistical channel knowledge which varies much slower than small-scale channel fading.

## 4. Optimization Design

Based on the deterministic equivalents derived in Section 3, an alternative sum-rate maximization problem is given as

$$\max_{\eta, r, \mathbf{P}^{(U)}} \bar{R}_{\text{sum}} \tag{23a}$$

$$\text{s.t. } \eta \bar{R}_{0,\text{sum}} \leq (1 - \eta) \bar{R}_{0,\text{bh}}, \tag{23b}$$

$$(12c), (12d), (12e). \tag{23c}$$

Note that the objective function and backhaul constraint are related to the statistical channel knowledge, thus, the redundant Monte Carlo averaging computation can be avoided. However, the optimal solution of the maximization problem (23) is still hard to find as the non-convexity of the objective function.

In the following, we first reformulate problem (23) as a minimization problem of two fractions added. The transmit power matrix of UAV  $\mathbf{P}^{(U)}$  is then analyzed in an independent sum-rate maximization problem. Finally, the solution to the placement problem is obtained using the first order Taylor approximation.

#### 4.1. Optimization of Bandwidth Allocation

According to the backhaul constraint, the optimal value of spectrum allocation  $\eta$  can be obtained when  $\eta\bar{R}_{0,\text{sum}} = (1 - \eta)\bar{R}_{0,\text{bh}}$ , thus we have

$$\eta^* = \frac{\bar{R}_{0,\text{bh}}}{(\bar{R}_{0,\text{sum}} + \bar{R}_{0,\text{bh}})}. \tag{24}$$

By substituting the optimal value of  $\eta$  into (23), we reformulate an equivalent problem as

$$\min_{r, \mathbf{P}^{(U)}} \frac{1}{\bar{R}_{0,\text{sum}}} + \frac{1}{\bar{R}_{0,\text{bh}}} \tag{25a}$$

$$\text{s.t. (12d), (12e)}. \tag{25b}$$

We observe that, in the equivalent minimization problem,  $\bar{R}_{0,\text{sum}}$  and  $\bar{R}_{0,\text{bh}}$  are separated in two fractions. Therefore, the transmit power matrix of the UAV can be analyzed in an independent sum-rate maximization problem.

#### 4.2. Optimization of Transmit Power Matrix

Based on the discussion in previous subsection, the transmit power matrix of the UAV  $\mathbf{P}^{(U)}$  can be solved by the following independent sum-rate maximization problem as

$$\max_{\mathbf{P}^{(U)}} \bar{R}_{0,\text{sum}} \tag{26a}$$

$$\text{s.t. (12e)}. \tag{26b}$$

This sum-rate maximization problem can be solved by the WMMSE algorithm described in References [24,25], where we define the equivalent channel  $\hat{h}_{kj} = \mathbf{h}_k^H \hat{\mathbf{w}}_j$ . Based on the deterministic equivalents proposed in Section 3, we have the corresponding deterministic equivalents of  $\hat{h}_{kk}$  and  $|\hat{h}_{kj}|^2$ , which are respectively given by

$$\hat{h}_{kk} - \frac{e_k}{1 + e_k} \sqrt{\frac{1}{\delta}} \rightarrow 0, \tag{27a}$$

$$|\hat{h}_{kj}|^2 - \frac{\beta}{d_k^\alpha M} \frac{e'_j}{(1 + e_j)^2} \rightarrow 0, \tag{27b}$$

as  $M \rightarrow \infty$ .

Note that with the consideration of RZF precoding regime, the equivalent channels of different UEs are almost equal, thus the near-optimal power allocation scheme is to allocate the total power to each UE equally.

### 4.3. Optimization of UAV Placement

Given the equal power allocation is adopted at the UAV, the problem (25) can be reformulated as the optimum placement problem given by

$$\min_r \frac{1}{\bar{R}_{0,\text{sum}}} + \frac{1}{\bar{R}_{0,\text{bh}}} \tag{28a}$$

$$\text{s.t. (12d)}. \tag{28b}$$

Note that  $R_{0,\text{sum}}$  is concave with respect to  $r$  [26,27], as the consistency of  $\bar{R}_{0,\text{sum}}$  and  $R_{0,\text{sum}}$  is verified in Section 5, thus,  $\bar{R}_{0,\text{sum}}$  is concave with respect to  $r$ . However,  $\bar{R}_{0,\text{bh}}$  is neither concave nor convex with respect to  $r$ . Thus, an approximation of  $\bar{R}_{0,\text{bh}}$  is introduced based on its first-order Taylor expansion. We achieve the approximation as followed.

Give a point  $r(n)$  in the  $n$ -th iteration. According to the first-order Taylor expansion at the given local point  $r(n)$ , we obtain the approximation  $\bar{R}_{0,\text{bh}}^{\text{appro}}$  as

$$\bar{R}_{0,\text{bh}}^{\text{appro}} = \frac{\partial \bar{R}_{0,\text{bh}}}{\partial r}(r(n)) (r - r(n)) + \bar{R}_{0,\text{bh}}(r(n)), \tag{29}$$

where  $\frac{\partial \bar{R}_{0,\text{bh}}}{\partial r}$  is the first-order derivative, which is given by

$$\frac{\partial \bar{R}_{0,\text{bh}}}{\partial r} = \frac{1}{\log 2} \left( \text{tr}(\mathbf{Y}^{-1} \frac{\partial \mathbf{Y}}{\partial r}) + N \left( \frac{-\frac{\partial \varphi}{\partial r}}{(1 + \varphi)^2} + \frac{\frac{\partial \varphi}{\partial r}}{1 + \varphi} \right) \right), \tag{30}$$

with

$$\frac{\partial \varphi}{\partial r} = \frac{-2rp_b\beta}{(r^2 + l^2)^2} \text{tr}(\mathbf{Y}^{-1}) - \frac{p_b\beta}{r^2 + l^2} \text{tr}(\mathbf{Y}^{-1} \frac{\partial \mathbf{Y}}{\partial r} \mathbf{Y}^{-1}), \tag{31a}$$

$$\frac{\partial \mathbf{Y}}{\partial r} = \frac{-Np_B\beta(2r(1 + \varphi) + (r^2 + l^2) \frac{\partial \varphi}{\partial r})}{(r^2 + l^2)^2(1 + \varphi)^2} \mathbf{I}_M. \tag{31b}$$

Then, with the given local point  $r(n)$  and the approximation  $\bar{R}_{0,\text{bh}}^{\text{appro}}$ , problem (28) can be approximated as

$$\min_r \frac{1}{\bar{R}_{0,\text{sum}}} + \frac{1}{\bar{R}_{0,\text{bh}}^{\text{appro}}} \tag{32a}$$

$$\text{s.t. (12d)}. \tag{32b}$$

Note that the problem (32) is a convex problem with the linear constraint, thus, it can be solved by some optimization tools, such as CVX [28]. Therefore, an iterative algorithm is proposed to find the solution of problem (32), which is shown in Algorithm 1.

---

#### Algorithm 1 Iterative Algorithm for Problem (32)

---

**Input:** Initial solution  $r(0)$  and tolerance factor  $\epsilon$ ;

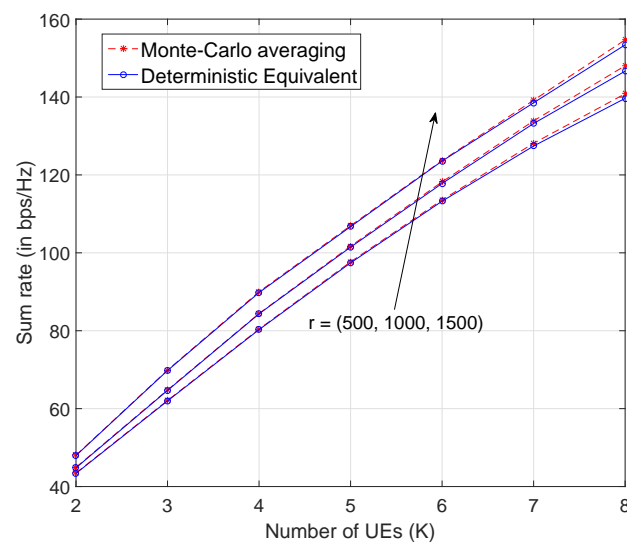
**Output:** optimal  $r^*$ .

- 1: **repeat**
  - 2:     Obtain  $e_k, \Psi, \varphi, \mathbf{Y}$  by solving (16) and (22) with  $r(n)$ ;
  - 3:     Obtain the approximation  $\bar{R}_{0,\text{bh}}^{\text{appro}}$  with  $r(n)$ ;
  - 4:     Find the solution  $r(n + 1)$  of problem (32);
  - 5:     Update  $n = n + 1$ ;
  - 6: **until** the residual of objective function is less than  $\epsilon$ .
-

## 5. Numerical Results and Discussion

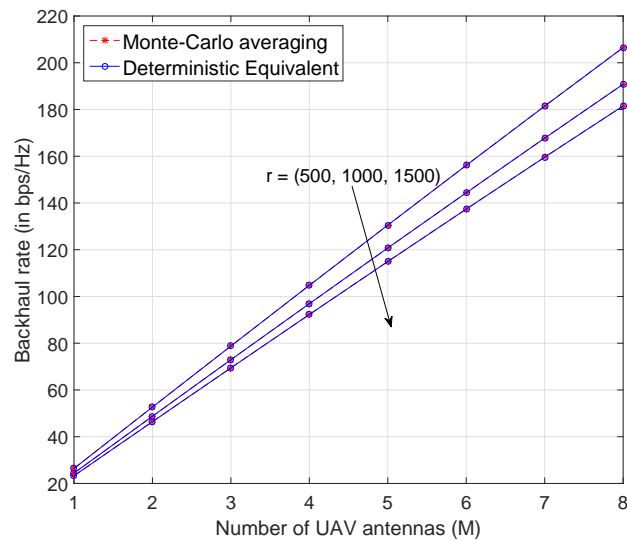
In this section, the accuracy of the deterministic equivalents of the ergodic sum-rate and wireless backhaul capacity are first verified, and then we use the deterministic equivalents to investigate the system performance and the effectiveness of the proposed algorithm. We consider a downlink UAV-assisted wireless communication network where a GBS is located at the origin with  $N = 12$  antennas. The UEs are randomly distributed in the region of  $z_k \in [2000, 2200]$  m, and  $\theta_k \in [0, \pi/2]$  with a uniform distribution under the polar coordinate. The height of the UAV  $l = 100$  m, the noise power is  $\sigma^2 = -110$  dBm, the path loss exponent  $\alpha = 2$ , and the channel power gains at the reference distance  $\beta = 0.1$  W [15,26].

In Figures 2–4, we compare the ergodic sum-rate of UEs  $R_{0,\text{sum}}$  and the ergodic capacity rate of the backhaul  $R_{0,\text{bh}}$  with their deterministic equivalents  $\bar{R}_{0,\text{sum}}, \bar{R}_{0,\text{bh}}$  under various system settings, respectively. Monte-Carlo simulation results is obtained by averaging over a large number of i.i.d. small-scale fading channels. The accuracy of the deterministic equivalents is validated even for practical system dimensions.



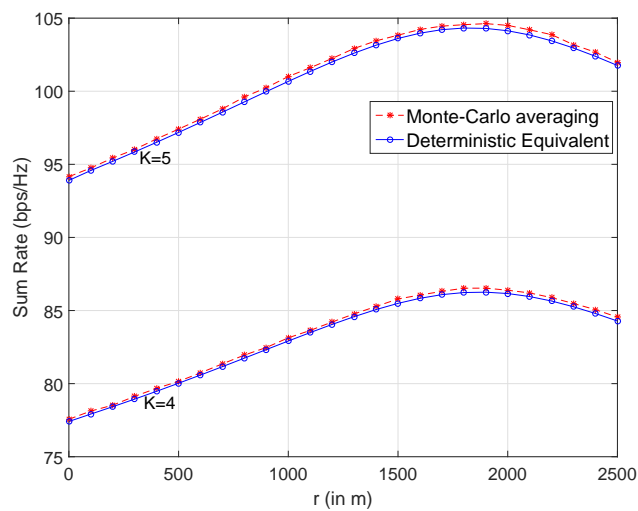
**Figure 2.** Comparison of ergodic sum-rate of UEs and the deterministic equivalent versus the number of UEs.

Figure 2 compares  $R_{0,\text{sum}}$  over the numbers of UEs with different values of the UAV's projection distance with  $\{M = 10, p_k = 0.2$  W,  $r = (500, 1000, 1500)$  m}. Owing to the RZF precoding, inter-user interference can be mitigated, thus, higher sum-rate can be achieved as the numbers of UEs grows. Moreover, the larger UAV's projection distance indicates the UAV is closer to the UEs and better channel condition can be obtained. Figure 3 shows the backhaul rate versus different numbers of UAV antennas with the fixed number  $\{N = 12\}$  of the GBS antennas. It states that the UAV with more number of antennas provides better performance due to higher multi-antenna gain, meanwhile, the larger UAV's projection distance results in less backhaul capacity.



**Figure 3.** Comparison of ergodic backhaul rate and the deterministic equivalent versus the number of UAV antennas.

Figure 4 illustrates the impact of UAV’s projection distance on  $R_{0,\text{sum}}$  with  $\{M = 10, p_k = 0.2 W, K = (4, 5)\}$ . The optimal sum-rate can be found as the UAV hovers approaching to the UEs. However, when the backhaul capacity constraint and the dynamic spectrum allocation are considered, the achievable rate of UEs’ access links and UAV’s backhaul link can be both affected by the placement of the UAV.



**Figure 4.** Comparison of ergodic sum-rate of UEs versus UAV’s projection distance.

The approximation problem (23) based on the deterministic equivalents is effective as the accuracy of the deterministic equivalents is verified. It can avoid complicated computation resulting from Monte-Carlo averaging over small-scale fading channels, and the optimization problem becomes a slow time-scale issue.

In Figure 5, we compare the optimal normalized sum-rate of UEs  $R_{\text{sum}}$  and the optimal UAV’s projection distance  $r$  with respect to the transmit power of the GBS under the scenario of  $\{N = 8, M = 6, K = 4, p_k = 0.2W\}$ . The optimal UAV’s projection distance is found by solving problem (32), and the optimal normalized sum-rate can be obtained, accordingly. The line corresponds to its coordinate with the same color. Figure 5 indicates that with the transmit power of the GBS

growing, the optimal UAV’s projection distance increases fast especially in the low GBS transmit power region, since the system performance is restricted by the backhaul capacity. The backhaul capacity becomes abundant when the transmit power of the GBS is large. Therefore, the UAV trends to approach to UEs where the higher rates of access links can be achieved. Note that the optimal UAV’s projection distance is determined by both the rates of access links and backhaul. The optimal normalized sum-rate also increases fast with the transmit power of the GBS grows, and then it will be degraded by the rates of access links.

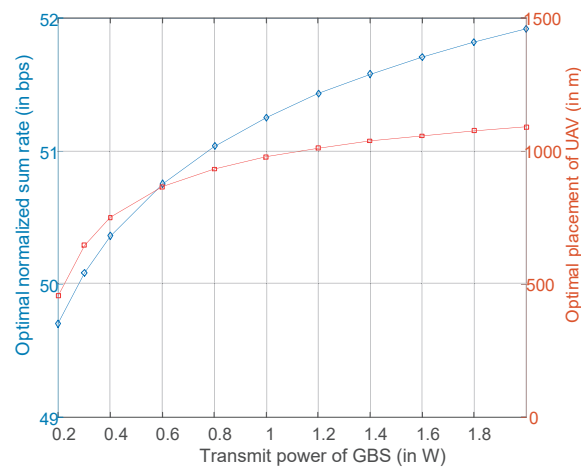


Figure 5. Optimal normalized sum-rate and optimal UAV’s projection distance versus GBS transmit power.

In Figure 6, it represents that the normalized sum-rate and the optimal spectrum allocation  $\eta$  are affected by the UAV’s projection distance with a fixed GBS transmit power  $p_b = 0.2 W$ . The line corresponds to the coordinate with the same color. From Figure 6, as the UAV is near to the GBS at the beginning, the backhaul capacity becomes dominant compared with the rates of access links. Therefore, less spectrum resource is allocated to the backhaul. With the UAV’s projection distance becomes large, the UAV is far away from the GBS, the limited backhaul capacity will significantly restrict the system performance. In order to satisfy the backhaul constraint, more spectrum resource will be designated to the backhaul.

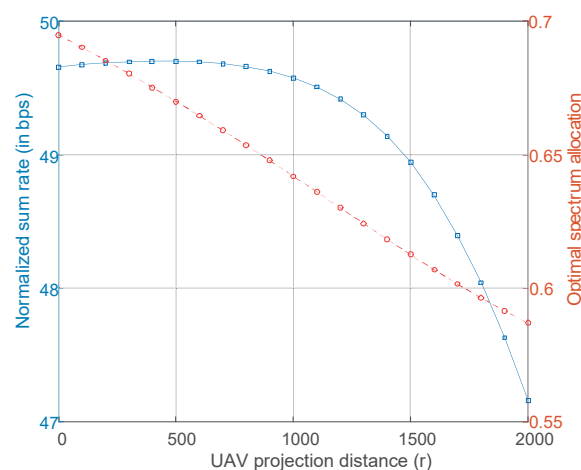


Figure 6. Normalized sum-rate and optimal spectrum allocation versus UAV’s projection distance.

Figure 7 illustrates that using the optimal dynamic spectrum resource allocation can achieve higher normalized sum-rate, as the optimal dynamic spectrum allocation factor always achieves the balance between the rates of backhaul and access links. When  $\eta = 0.5$ , the normalized sum-rate is always less than that of backhaul. As  $\eta = 0.6$ , more spectrum resource is allocated to the access links,

and the normalized sum-rate is larger than that of backhaul when the UAV's projection distance is large where the UAV is near the UEs. Therefore, the normalized sum-rate is then degraded by the normalized backhaul rate in this case.

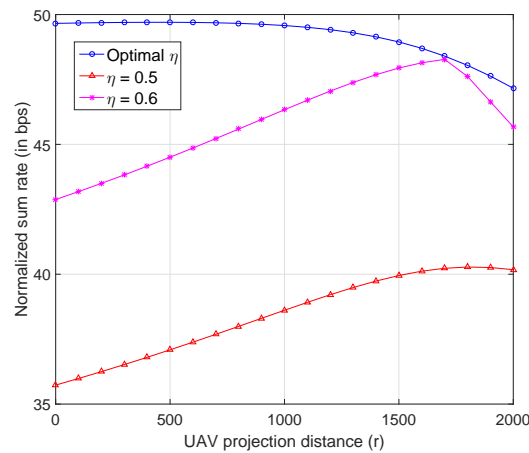


Figure 7. Normalized sum-rate versus UAV's projection distance with different spectrum allocation.

Figure 8 presents the convergence performance of proposed algorithm with respect to the residual norm which is defined as the norm of the difference between the  $n$ -th iterative and the prior iterative value of the objective function. The tolerance  $\epsilon$  is set as  $10^{-3}$ , and we consider the scenarios under different number of users and UAV's antennas which are labeled in the figure. From the figure, it indicates that the residual norm will convergence to zero after a few number of iterations for different numbers of users and UAV's antennas, as a result, the proposed algorithm ensures a fast convergence.

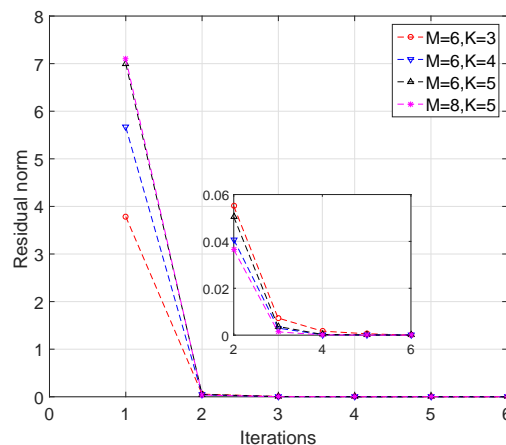


Figure 8. Convergence performance of the proposed algorithm with different number of users and UAV's antennas.

## 6. Conclusions

In this paper, we considered a UAV-assisted wireless communication network where a multi-antenna UAV utilized as a remote relay, assisted the GBS to forward signals for UEs in remote areas outside the coverage of the GBS. The UAV was connected to the GBS through in-band wireless backhaul, which shared the spectrum resource with the access links of UEs due to the limited spectrum resource. To mitigate the inter-user interference, the RZF precoding was adopted. A sum-rate maximization problem was formulated by jointly designing the spectrum resource allocation factor, the UAV's projection distance, and the transmit power matrix at the UAV. The deterministic equivalents

of the ergodic sum-rate and wireless backhaul capacity were derived using large dimensional random matrix theory. Based on the deterministic equivalents, an approximation problem of the original optimization problem was formulated and the suboptimal solutions were obtained. The simulation results validated the accuracy of the deterministic equivalents and showed the system performance with respect to different variables, that is, the user number, the number of the UAV antennas, the transmit power of the GBS, and UAV projection distance.

In this work, the elastic UAV was deployed to assist the static terrestrial network. How to utilize the UAV to serve dynamic network is still an open issue. In addition, due to the on-board battery of the UAV is limited, the energy efficiency problem of the UAV-assisted network is still a challenge which needs more efforts in future research.

**Author Contributions:** Conceptualization, Y.X., W.X. and J.Z.; methodology, Y.X., J.Z.; software, Y.X., B.X.; validation, W.X.; formal analysis, Y.X.; investigation, Y.X.; writing—original draft preparation, Y.X.; writing—review and editing, Y.X., W.X.; visualization, Y.X.; supervision, J.Z.; project administration, H.Z.; funding acquisition, H.Z. All authors have read and agreed to the published version of the manuscript.

**Funding:** This research was funded by the National Natural Science Foundation of China under Grant U1805262, 61871446, and 61671251.

**Conflicts of Interest:** The authors declare no conflict of interest. The funders had no role in the design of the study; in the collection, analyses, or interpretation of data; in the writing of the manuscript, or in the decision to publish the results.

### Appendix A. Proof of Lemma 1

By substituting (5) into (8), we obtain

$$\gamma_k = \frac{p_k^{(U)} |\mathbf{h}_k^H \mathbf{A}^{-1} \mathbf{h}_k|^2}{\sum_{j=1, j \neq k}^K p_j^{(U)} |\mathbf{h}_k^H \mathbf{A}^{-1} \mathbf{h}_j|^2 + \sigma^2 / \xi^2}, \quad (\text{A1})$$

where we define  $\mathbf{A} = \mathbf{A}_{[k]} + \mathbf{h}_k \mathbf{h}_k^H$  and  $\mathbf{A}_{[k]} = \mathbf{H}_{[k]} \mathbf{H}_{[k]}^H + \omega \mathbf{I}_M$ .  $\mathbf{H}_{[k]}$  is the channel matrix except the  $k$ -th column, and  $\mathbf{H}_{[k]} = [\mathbf{h}_1, \dots, \mathbf{h}_{k-1}, \mathbf{h}_{k+1}, \dots, \mathbf{h}_K] \in \mathbb{C}^{M \times (K-1)}$ .

The SINR  $\gamma_k$  consists of three terms, including desired signal, interference, and noise part. The deterministic equivalents are derived for each term respectively.

By using matrix inverse lemma and the definition of  $\mathbf{A}$ , the term of desired signal can be written as

$$\mathbf{h}_k^H (\mathbf{A}_{[k]} + \mathbf{h}_k \mathbf{h}_k^H)^{-1} \mathbf{h}_k = \frac{\mathbf{h}_k^H \mathbf{A}_{[k]}^{-1} \mathbf{h}_k}{1 + \mathbf{h}_k^H \mathbf{A}_{[k]}^{-1} \mathbf{h}_k}. \quad (\text{A2})$$

Based on the definition of  $\mathbf{h}_k$ , we have  $\mathbf{h}_k^H \mathbf{A}_{[k]}^{-1} \mathbf{h}_k$  almost surely converges to  $\frac{\beta}{a_k^{\alpha} M} \text{tr}(\mathbf{A}_{[k]}^{-1})$ . According to the fact that  $\frac{1}{M} \text{tr}(\mathbf{A}_{[k]}^{-1}) - \frac{1}{M} \text{tr}(\mathbf{A}^{-1}) \rightarrow 0$ , almost surely, and [27] [Theorem 1], we obtain  $\mathbf{h}_k^H \mathbf{A}_{[k]}^{-1} \mathbf{h}_k - e_k \rightarrow 0$ , where  $e_k$  is given by (16a). Thus, we have the deterministic equivalent of the signal part is

$$\mathbf{h}_k^H \mathbf{A}^{-1} \mathbf{h}_k - \frac{e_k}{1 + e_k} \rightarrow 0, \quad (\text{A3})$$

as  $M \rightarrow \infty$ .

According to (6), the term of  $\frac{1}{\xi^2}$  is given by

$$\frac{1}{\xi^2} = \text{tr} \left[ \mathbf{H}^H (\mathbf{H} \mathbf{H}^H + \omega \mathbf{I}_M)^{-2} \mathbf{H} \right]. \quad (\text{A4})$$

By using matrix inverse lemma twice, the term of  $\frac{1}{\xi^2}$  can be written as

$$\frac{1}{\xi^2} = \sum_{k=1}^K \frac{\mathbf{h}_k^H \mathbf{A}_{[k]}^{-2} \mathbf{h}_k}{(1 + \mathbf{h}_k^H \mathbf{A}_{[k]}^{-1} \mathbf{h}_k)^2}. \tag{A5}$$

Similar to the signal part, by using the fact that  $\frac{1}{M} \text{tr}(\mathbf{A}_{[k]}^{-1}) - \frac{1}{M} \text{tr}(\mathbf{A}^{-1}) \rightarrow 0$ , almost surely, and [27] [Theorem 1], we obtain  $\mathbf{h}_k^H \mathbf{A}_{[k]}^{-1} \mathbf{h}_k - e_k \rightarrow 0$  and  $\mathbf{h}_k^H \mathbf{A}_{[k]}^{-2} \mathbf{h}_k - e'_k \rightarrow 0$ , thus, we have the deterministic equivalent of  $\frac{1}{\xi^2}$  as

$$\frac{1}{\xi^2} - \frac{1}{M} \sum_{k=1}^K \frac{e'_k}{(1 + e_k)^2} \rightarrow 0, \tag{A6}$$

as  $M \rightarrow \infty$ , where the term  $e'_k$  is the derivative of  $e_k$  and derived by

$$e'_k = \frac{\beta}{d_k^\alpha M} \text{tr} \left( \frac{1}{M} \sum_{j=1}^K \frac{\beta e'_j}{d_j^\alpha (1 + e_j)^2} \mathbf{\Psi}^2 \right) + \frac{\beta}{d_k^\alpha M} \text{tr} (\mathbf{\Psi}^2). \tag{A7}$$

Define  $\mathbf{e}' = [e'_1, \dots, e'_K]^T$  which forms the equation  $\mathbf{e}' = \mathbf{J}\mathbf{e}' + \mathbf{v}$ . The solution is given in (19).

The interference part can be rewritten as  $\mathbf{h}_k^H \mathbf{A}^{-1} \mathbf{H}_{[k]} \mathbf{P}_{[k]} \mathbf{H}_{[k]}^H \mathbf{A}^{-1} \mathbf{h}_k$  based on (5), where  $\mathbf{H}_{[k]} = [\mathbf{h}_1, \dots, \mathbf{h}_{k-1}, \mathbf{h}_{k+1}, \dots, \mathbf{h}_K]$ , and  $\mathbf{P}_{[k]} = \text{diag}(p_1, \dots, p_{k-1}, p_{k+1}, \dots, p_K)$ , we have

$$\begin{aligned} & \mathbf{h}_k^H \mathbf{A}^{-1} \mathbf{H}_{[k]} \mathbf{P}_{[k]} \mathbf{H}_{[k]}^H \mathbf{A}^{-1} \mathbf{h}_k \\ &= \mathbf{h}_k^H \mathbf{A}_{[k]}^{-1} \mathbf{H}_{[k]} \mathbf{P}_{[k]} \mathbf{H}_{[k]}^H \mathbf{A}^{-1} \mathbf{h}_k \\ &+ \mathbf{h}_k^H (\mathbf{A}^{-1} - \mathbf{A}_{[k]}^{-1}) \mathbf{H}_{[k]} \mathbf{P}_{[k]} \mathbf{H}_{[k]}^H \mathbf{A}^{-1} \mathbf{h}_k. \end{aligned} \tag{A8}$$

By using  $\mathbf{A}^{-1} - \mathbf{A}_{[k]}^{-1} = -\mathbf{A}^{-1}(\mathbf{A} - \mathbf{A}_{[k]})\mathbf{A}_{[k]}^{-1}$ , we obtain

$$\begin{aligned} & \mathbf{h}_k^H \mathbf{A}^{-1} \mathbf{H}_{[k]} \mathbf{P}_{[k]} \mathbf{H}_{[k]}^H \mathbf{A}^{-1} \mathbf{h}_k \\ &= \mathbf{h}_k^H \mathbf{\Phi} \mathbf{h}_k - \mathbf{h}_k^H \mathbf{A}^{-1} \mathbf{h}_k \mathbf{h}_k^H \mathbf{\Phi} \mathbf{h}_k, \end{aligned} \tag{A9}$$

where  $\mathbf{\Phi} = \mathbf{A}_{[k]}^{-1} \mathbf{H}_{[k]} \mathbf{P}_{[k]} \mathbf{H}_{[k]}^H \mathbf{A}^{-1}$ . By applying [27] [Lemma 7], we have

$$\begin{aligned} & \mathbf{h}_k^H \mathbf{A}^{-1} \mathbf{h}_k - \frac{u}{1 + u} \rightarrow 0, \\ & \mathbf{h}_k^H \mathbf{\Phi} \mathbf{h}_k - \frac{\chi}{1 + u} \rightarrow 0, \end{aligned} \tag{A10}$$

where  $u = \frac{\beta}{d_k^\alpha M} \text{tr}(\mathbf{A}_{[k]}^{-1})$  and  $\chi = \frac{\beta}{d_k^\alpha M} \text{tr}(\mathbf{P}_{[k]} \mathbf{H}_{[k]}^H \mathbf{A}_{[k]}^{-2} \mathbf{H}_{[k]})$ . Using the fact that  $\frac{1}{M} \text{tr}(\mathbf{A}_{[k]}^{-1}) - \frac{1}{M} \text{tr}(\mathbf{A}^{-1}) \rightarrow 0$ , we rewrite  $\chi$  as

$$\chi = \frac{\beta}{d_k^\alpha M} \sum_{j=1, j \neq k}^K p_j \mathbf{h}_j^H \mathbf{A}^{-2} \mathbf{h}_j. \tag{A11}$$

By using matrix inverse lemma and [27] [Theorem 1], we obtain

$$\mathbf{h}_k^H \mathbf{A}^{-1} \mathbf{h}_k - \frac{e_k}{1 + e_k} \rightarrow 0, \tag{A12a}$$

$$\mathbf{h}_k^H \Phi \mathbf{h}_k - \frac{\frac{\beta}{d_k^\alpha M} \sum_{j=1, j \neq k}^K p_j \frac{e'_j}{(1+e_j)^2}}{1 + e_k} \rightarrow 0. \tag{A12b}$$

Substituting (A12a) and (A12b) into (A9), the deterministic equivalent of the interference part is

$$\sum_{j=1, j \neq k}^K p_j^{(U)} \left| \mathbf{h}_k^H \mathbf{A}^{-1} \mathbf{h}_j \right|^2 - \frac{\frac{\beta}{d_k^\alpha M} \sum_{j=1, j \neq k}^K p_j \frac{e'_j}{(1+e_j)^2}}{(1 + e_k)^2} \rightarrow 0, \tag{A13}$$

as  $M \rightarrow \infty$ .

Substituting the deterministic equivalents of desired signal, interference, and noise part into (8), then the deterministic equivalent of the SINR  $\gamma_k$  is obtained in Lemma 1, hence the proof is completed.

### Appendix B. Proof of Lemma 2

We consider that  $R_{0,bh}(\sigma^2)$  is a function of  $\sigma^2$ . The derivative of  $R_{0,bh}(\sigma^2)$  with respect to  $\sigma^2$  is expressed as

$$\begin{aligned} & \frac{\partial R_{0,bh}(\sigma^2)}{\partial \sigma^2} \\ &= \frac{1}{\log 2} \left\{ \mathbb{E} \left[ \text{tr} \left( \mathbf{G} \mathbf{P}^{(B)} \mathbf{G}^H + \sigma^2 \mathbf{I}_M \right)^{-1} \right] - \frac{M}{\sigma^2} \right\}. \end{aligned} \tag{A14}$$

The mutual information can be equivalently written as [23]

$$\begin{aligned} & R_{0,bh}(\sigma^2) \\ &= \frac{1}{\log 2} \int_{-\infty}^{\sigma^2} \left\{ \mathbb{E} \left[ \text{tr} \left( \mathbf{G} \mathbf{P}^{(B)} \mathbf{G}^H + \vartheta \mathbf{I}_M \right)^{-1} \right] - \frac{M}{\vartheta} \right\} d\vartheta. \end{aligned} \tag{A15}$$

Utilizing the large dimensional random matrix theory, we obtain

$$\text{tr} \left( \mathbf{G} \mathbf{P}^{(B)} \mathbf{G}^H + v \mathbf{I}_M \right)^{-1} - \text{tr}(\mathbf{Y})^{-1} \rightarrow 0, \tag{A16}$$

as  $M \rightarrow \infty$ , where  $\mathbf{Y}$  is given by (22). We define  $\Omega = \frac{p_b \beta}{d_u} \mathbf{I}_M$  and  $R(\sigma^2, x)$  given by

$$\begin{aligned} & R(\sigma^2, x) \\ &= \frac{1}{\log 2} \left[ \log \det(Nx\Omega + \sigma^2 \mathbf{I}_M) + N(x - \log x) - M \log \sigma^2 \right]. \end{aligned} \tag{A17}$$

The explicit expression can be proved according to References [23], as

$$\frac{\partial R_{0,bh}(\sigma^2)}{\partial \sigma^2} = \frac{\partial R}{\partial \sigma^2} \Big|_{x=\frac{1}{1+\varphi}}, \tag{A18}$$

where  $\varphi$  is given by (22), hence the proof is completed.

## References

1. Mozaffari, M.; Saad, W.; Bennis, M.; Debbah, M. Efficient deployment of multiple unmanned aerial vehicles for optimal wireless coverage. *IEEE Trans. Wirel. Commun.* **2016**, *15*, 3949–3963. [[CrossRef](#)]
2. Zeng, Y.; Zhang, R.; Lim, T. Wireless communications with unmanned aerial vehicles: Opportunities and challenges. *IEEE Commun. Mag.* **2016**, *54*, 36–42. [[CrossRef](#)]
3. Zhang, S.; Zeng, Y.; Zhang, R. Cellular-enabled UAV communication: A connectivity-constrained trajectory optimization perspective. *IEEE Trans. Commun.* **2019**, *67*, 2580–2604. [[CrossRef](#)]
4. Kalantari, E.; Shakir, M.; Yanikomeroglu, H.; Yongacoglu, A. Backhaul-aware robust 3D drone placement in 5G+ wireless networks. In Proceedings of the 2017 IEEE International Conference on Communications Workshops (ICC Workshops), Paris, France, 21–25 May 2017; pp. 109–114.
5. Galkin, B.; Kibilda, J.; DaSilva, L. Backhaul for low-altitude UAVs in urban environments. In Proceedings of the 2018 IEEE International Conference on Communications (ICC), Kansas City, MO, USA, 20–24 May 2018; pp. 1–6.
6. Qiu, C.; Wei, Z.; Feng, Z.; Zhang, P. Joint resource allocation, placement and user association of multiple UAV-mounted base stations with in-band wireless backhaul. *IEEE Wirel. Commun. Lett.* **2016**, *15*, 3949–3963. [[CrossRef](#)]
7. Youssef, M.; Nour, C.A.; Farah, J.; Douillard, C. Backhaul-constrained resource allocation and 3D placement for UAV-enabled networks. In Proceedings of the 2019 IEEE 90th Vehicular Technology Conference (VTC2019-Fall), Honolulu, HI, USA, 22–25 September 2019; pp. 1–7.
8. Wu, Q.; Zeng, Y.; Zhang, R. Joint trajectory and communication design for multi-UAV enabled wireless networks. *IEEE Trans. Wirel. Commun.* **2018**, *17*, 2109–2121. [[CrossRef](#)]
9. Zeng, Y.; Xu, J.; Zhang, R. Energy minimization for wireless communication with rotary-wing UAV. *IEEE Trans. Wirel. Commun.* **2019**, *18*, 2329–2345. [[CrossRef](#)]
10. Chen, Y.; Feng, W.; Zheng, G. Optimum placement of UAV as relays. *IEEE Commun. Lett.* **2018**, *22*, 248–251. [[CrossRef](#)]
11. Lyu, J.; Zeng, Y.; Zhang, R.; Lim, T.J. Placement optimization of UAV-mounted mobile base stations. *IEEE Commun. Lett.* **2017**, *21*, 604–607. [[CrossRef](#)]
12. Wu, H.; Tao, X.; Zhang, N.; Shen, X. Cooperative UAV cluster-assisted terrestrial cellular networks for ubiquitous coverage. *IEEE J. Sel. Areas Commun.* **2018**, *36*, 2045–2058. [[CrossRef](#)]
13. Zhan, C.; Zeng, Y.; Zhang, R. Energy-efficient data collection in UAV enabled wireless sensor network. *IEEE Wirel. Commun. Lett.* **2018**, *7*, 328–331. [[CrossRef](#)]
14. Xia, W.; Zhang, J.; Jin, S.; Wen, C.; Gao, F.; Zhu, H. Large system analysis of resource allocation in heterogeneous networks with wireless backhaul. *IEEE Trans. Commun.* **2017**, *65*, 5040–5053. [[CrossRef](#)]
15. Feng, W.; Wang, J.; Chen, Y.; Wang, X.; Ge, N.; Lu, J. UAV-aided MIMO communications for 5G Internet of Things. *IEEE Internet Things J.* **2019**, *6*, 1731–1740. [[CrossRef](#)]
16. Song, Q.; Zheng, F.; Zeng, Y.; Zhang, J. Joint beamforming and power allocation for UAV-enabled full-duplex relay. *IEEE Trans. Veh. Technol.* **2019**, *68*, 1657–1671. [[CrossRef](#)]
17. Shen, Y.; Pan, Z.; Liu, N.; You, X. Joint design and performance analysis of a full-duplex UAV legitimate surveillance system. *Electronics* **2020**, *9*, 407. [[CrossRef](#)]
18. Motlagh, N.; Taleb, T.; Arouk, O. Low-altitude unmanned aerial vehicles-based Internet of Things services: Comprehensive survey and future perspectives. *IEEE Internet Things J.* **2016**, *3*, 899–922. [[CrossRef](#)]
19. Zhang, J.; Wen, C.; Jin, S.; Gao, X.; Wong, K.K. Large system analysis of cooperative multi-cell downlink transmission via regularized channel inversion with imperfect CSIT. *IEEE Trans. Wirel. Commun.* **2013**, *12*, 4801–4813. [[CrossRef](#)]
20. Xia, W.; Zhang, J.; Quek, T.Q.S.; Jin, S.; Zhu, H. Joint optimization of fronthaul compression and bandwidth allocation in uplink H-CRAN with large system analysis. *IEEE Trans. Commun.* **2018**, *66*, 6556–6569. [[CrossRef](#)]
21. Xue, Y.; Zhang, J.; Jin, S.; Zheng, G.; Zhu, H. Large system analysis of downlink C-RAN with phase noise and fronthaul compression. *China Commun.* **2019**, *16*, 58–71. [[CrossRef](#)]
22. Peel, C.B.; Hochwald, B.M.; Swindlehurst, A.L. A vector-perturbation technique for near-capacity multiantenna multiuser communication—Part I: Channel inversion and regularization. *IEEE Trans. Commun.* **2005**, *53*, 195–202. [[CrossRef](#)]

23. Wen, C.; Pan, G.; Wong, K.; Guo, M.; Chen, J. A deterministic equivalent for the analysis of non-gaussian correlated MIMO multiple access channels. *IEEE Trans. Inf. Theory* **2013**, *59*, 329–352. [[CrossRef](#)]
24. Shi, Q.; Razaviyayn, M.; Luo, Z.; He, C. An iteratively weighted MMSE approach to distributed sum-utility maximization for a MIMO interfering broadcast channel. *IEEE Trans. Signal Process.* **2011**, *59*, 4331–4340. [[CrossRef](#)]
25. Sun, H.; Chen, X.; Shi, Q.; Hong, M.; Fu, X.; Sidiropoulos, N.D. Learning to optimize: Training deep neural networks for wireless resource management. In Proceedings of the 2017 IEEE 18th International Workshop on Signal Processing Advances in Wireless Communications (SPAWC), Sapporo, Japan, 3–6 July 2017; pp. 1–6.
26. Pan, C.; Yi, J.; Yin, C.; Yu, J.; Li, X. Joint 3D UAV placement and resource allocation in software-defined cellular networks with wireless backhaul. *IEEE Access* **2019**, *7*, 104279–104293. [[CrossRef](#)]
27. Wagner, S.; Couillet, R.; Debbah, M.; Slock, D.T.M. Large system analysis of linear precoding in correlated MISO broadcast channels under limited feedback. *IEEE Trans. Inf. Theory* **2012**, *58*, 4509–4537. [[CrossRef](#)]
28. Boyd, S.; Vandenberghe, L. *Convex Optimization*; Cambridge University Press: Cambridge, UK, 2004.



© 2020 by the authors. Licensee MDPI, Basel, Switzerland. This article is an open access article distributed under the terms and conditions of the Creative Commons Attribution (CC BY) license (<http://creativecommons.org/licenses/by/4.0/>).